O VI Observations of Galaxy Clusters: Evidence for Modest Cooling Flows

Joel N. Bregman[1], A.C. Fabian[2], Eric D. Miller[3], and Jimmy A. Irwin[1]

jbregman@umich.edu

ABSTRACT

A prediction of the galaxy cluster cooling flow model is that as gas cools from the ambient cluster temperature, emission lines are produced in gas at subsequently decreasing temperatures. Gas passing through $10^{5.5}$ K emits in the lines of O VI $\lambda\lambda$1032, 1035, and here we report a *FUSE* study of these lines in three cooling flow clusters, Abell 426, Abell 1795, and AWM 7. No emission was detected from AWM 7, but O VI is detected from the centers of Abell 426 and Abell 1795, and possibly to the south of the center in Abell 1795, where X-ray and optical emission line filaments lie. In Abell 426, these line luminosities imply a cooling rate of 32$\pm$6 $M_\odot$ yr^{-1} within the central r = 6.2 kpc region, while for Abell 1795, the central cooling rate is 26$\pm$7 $M_\odot$ yr^{-1} (within r = 22 kpc), and about 42$\pm$9 $M_\odot$ yr^{-1} including the southern pointing.

Including other studies, three of six clusters have O VI emission, and they also have star formation as well as emission lines from 10^4 K gas. These observations are generally consistent with the cooling flow model but at a rate closer to 30 $M_\odot$ yr^{-1} than originally suggested values of 10^2–10^3 $M_\odot$ yr^{-1}.

Subject headings: galaxies: clusters: individual (Abell 426, Abell 1795, AWM7) — cooling flows — ultraviolet: galaxies

1. Introduction

Before the launch of *XMM-Newton* and *Chandra*, the X-ray data provided strong support for the model of cooling flows (Fabian 1994). The X-ray imaging data of galaxy clusters

[1]Department of Astronomy, University of Michigan, Ann Arbor, MI 48109

[2]Institute of Astronomy, Madingley Road, Cambridge CB3 0HA

[3]Kavli Institute for Astrophysics and Space Science, MIT, Cambridge, MA 02139

showed a temperature decrease into the centers of these systems, typically by a factor of two from the ambient temperature of about 4-10 keV (5-12$\times10^7$ K). Within the inner 100 kpc, the radiative cooling times for the hot gas is shorter than a Hubble time, leading to the apparent inevitability that the gas would radiatively cool to much lower temperatures, and this is the basis of the cooling flow model with cooling rates of 30-1000 $M_\odot$ yr^{-1}. However, the existence of cooling flows has often been questioned by observers in other wavebands, who find some evidence for cooled gas and star formation, but at a level far below the rate inferred from the X-ray data (McNamara & O'Connell 1989, 1993; Cardiel et al. 1998).

Consequently, it was anticipated that *XMM* grating spectra would show strong emission from gas that was well below the ambient temperature of the medium, representing the substantial amounts of cooling gas. While the *XMM* data showed the expected luminosities of the high ionization line, such as Fe XXI to Fe XXIV, the emission from the lines that trace cooler gas were missing (e.g., Fe XVII, O VII; Peterson et al. 2003). According to these line ratios, the gas was not obviously cooling below about 2 keV (2.3×10^7 K). Either some heating mechanism turns on at 2 keV, preventing the gas from cooling further, or the gas continues to cool but these lines are not produced, due to metal inhomogenieties, turbulent mixing with cooler gas, or heating by AGNs (Fabian et al. 2001).

There is still good evidence for significantly cooler gas (e.g., 10^4 K gas in Perseus), which may be the end product of the cooling flow (Cowie et al. 1983; Hu et al. 1983, 1985; Ferruit et al. 1997; Conselice et al. 2001). However, unless one can find gas at temperatures between 10^4 K and 10^7 K, we would have to consider an alternative picture for the cooler gas, where it is mass lost from galaxies (Sparks et al. 1997). A particularly good tracer of cooling gas is the O VI $\lambda\lambda$ 1032, 1038 doublet, because it dominates the radiative cooling function where it is present ($\sim 10^{5.5}$ K), it cannot be produced by photoionization by stars, and it lies above 912 Å, so it is accessible with the *Far Ultraviolet Spectroscopic Explorer* (*FUSE*). This line has been detected in Abell 2597 by Oegerle et al. (2001) where they report a cooling rate of about 40 $M_\odot$ yr^{-1} within the inner 36 kpc of the cluster. They also report a nondetection, for Abell 1795, and Lecavelier des Etangs et al. (2004) report nondetections for Abell 2029 and Abell 3112. Here we report on *FUSE* observations of Abell 426 (the Perseus cluster), Abell 1795 (off-center observations), and AWM 7, all clusters that are bright in X-rays and originally expected to contain cooling flows. We find evidence for O VI emission from Perseus and Abell 1795 and discuss the importance of these observations in light of X-ray and other related observations. We use a Hubble constant of 70 km s^{-1} Mpc^{-1}.

2. Observations

All of the *FUSE* observations were obtained with the large aperture (30″ square; *LWRS*) in time-tag mode. The observations were screened for particle outbursts, with the resulting good data separated into day and night components. Each individual detector segment for each observation was combined using the procedure TTAG_COMBINE before applying the CALFUSE pipeline (origianally, version 2.4 was used but we also tried version 3.0, which led to no noticable changes for the spectral region of interest). For observations obtained during the day, the background is significantly higher than for observations taken at night. The background is composed of a combination of discrete airglow lines (e.g., from Hβ, O I, N_2) plus a diffuse scattered component. For the data taken during the day, this background is often stronger than the weak signals that we seek, so we usually used the data obtained during nighttime (discussed separately for each of our targets). For the Perseus cluster and AWM 7, the redshifted O VI doublet falls near 1050 Å, and in this regions the channel with the highest S/N is the LiF1a. As the addition of other channels reduces the S/N, we discuss only the LiF1a data for these clusters. For Abell 1795, the O VI line is shifted into the 1095–1098 Å region, where the only useful detector is the LiF2a channel. For purposes of displaying the data, the spectra are binned and smoothed, although for the extraction of line fluxes, the unsmoothed data were used.

2.1. Abell 426 (Perseus Cluster)

This is one of the most frequently observed clusters and it was one of the most compelling cases for cooling flows, as it showed an X-ray surface brightness distribution with a sharply peaked diffuse emission, extensive filaments from 10^4 K gas, and ongoing star formation (Norgaard-Nielsen et al. 1990; McNamara et al. 1996; Sanders et al. 2004). It also hosts an AGN with strong extended radio emission (3C 84) and the central object has been listed as a Seyfert 1.5 galaxy as well as a BL Lac type object. In addition to the central dominant galaxy, NGC 1275, at a redshift of 5264 km s^{-1}, there is a higher velocity gaseous component, at about 8200 km s^{-1} (first noted by Minkowski 1955), which contains warm ionized gas, neutral gas, and molecular gas (Jaffe 1990; Donahue et al. 2000; Krabbe et al. 2000). The emission line gas is seen over a 6′ diameter region, which is similar in size to the cooling radius of the X-ray emission (Conselice et al. 2001). Consequently, only a fraction of the cooling gas may be contained in the LWRS (30″ square centered on NGC 1275; Figure 1), so we may be missing a considerable amount of cooling gas, although this pointing contains the brightest Hα emitting gas and X-ray emitting gas. The data were taken in 16 October 2002, with a total exposure time of 29.1 ksec, of which 13.0 ksec is night data, used in our

analysis.

Several emission lines are detected, including Lyβ and both O VI lines near the redshift of NGC 1275 (Figure 2). The analysis of these lines is complicated by a variety of absorption lines, mostly from the Galaxy, but also from material within the Perseus cluster. From the Milky Way, we see strong absorption lines from H_2 in addition to the usual atomic lines, but this is to be expected given the low Galactic latitude and high extinction in this direction ($A_B = 0.70$ mag; Schlegel, Finkbeiner, and Davis 1998). This absorption affects the strong O VI λ 1032 line, which is absorbed on its blue and red sides by Galactic H_2. In addition, there is absorption due to H_2 from the higher redshift system in Perseus (8200 km s^{-1}), but this is to be expected as molecular gas was previously known to exist at this velocity (Jaffe 1990). Fortunately, no strong absorption features occur near the weaker O VI line, so we are able to obtain a line flux. For the O VI λ 1038 line, the flux is 2.9×10^{-15} erg cm^{-2} s^{-1} ($\pm$ 0.4×10^{-15} erg cm^{-2} s^{-1}), the line center is at 1055.9 $\pm$ 0.1 Å, and the width is 0.7 $\pm$ 0.2 Å (FWHM), while for the 1032 Å line, the flux is 2.9×10^{-15} erg cm^{-2} s^{-1} , which we regard as a lower limit due to the absorption. It is difficult to correct the strong line for absorption in a reliable manner, so we use the line ratio (of 2:1) and the strength of the λ 1038 line to infer the strength of the stronger line to be about 5.8×10^{-15} erg cm^{-2} s^{-1} ($\pm$ 0.9×10^{-15} erg cm^{-2} s^{-1}). After making an extinction correction, F(λ 1032) = 4.2 $\times$ 10-14 erg cm^{-2} s^{-1} ($\pm$ 0.6×10^{-14} erg cm^{-2} s^{-1}), and for a distance of 75.2 Mpc, the luminosity in the λ 1032 line is 2.9×10^{40} erg s^{-1} ($\pm$ 0.4×10^{40} erg s^{-1}. In addition, the Lyβ line is detected in emission, which was expected since Lyα was detected previously.

2.2. Abell 1795

The cluster has a mean redshift z = 0.062476 $\pm$ 0.00030 (Oegerle & Hill 2001) and the velocity dispersion of the cluster is 810 km s^{-1} ($\triangle$z = 0.0027). The velocity of the central dominant galaxy is slightly higher, at z = 0.06326. This cluster has a filament that extends about 40″ to the south of the central dominant galaxy and is detected in both optical emission line gas as well as diffuse X-rays (Hu et al. 1985; Fabian et al. 2001). The filament is at least a factor of two cooler than the ambient cluster gas and the radiative cooling time is 3 $\times$ 10^8 yr, about the age inferred from its length and velocity. We obtained an observation at this off-center location with the LWRS (30″ south of the CD galaxy), and in addition, we reanalyzed the central pointing (originally discussed by Oegerle et al. 2001), which contains the central dominant galaxy, the peak of the X-ray emission, and a significant fraction of the 10^4 K gas. The total exposure time of the central pointing is 37.1 ksec, of which 17.0 ksec were useful nighttime data, and those are the observations used below.

The central galaxy has an apparent magnitude of 15.2, so if the ratio of V to FUV flux was typical for an early-type galaxy (e.g., NGC 5846), the flux near 1115 Å (1050 Å in the rest frame) would have been about 5×10^{-16} erg cm^{-2} s^{-1} (after Bregman et al. 2005), but the observed flux is 2.7×10^{-15} erg cm^{-2} s^{-1}, about five times larger (Figure 3). There is a range in the FUV to V flux of early-type galaxies (Burstein et al. 1988), and some luminous galaxies are a magnitude brighter in their FUV flux (e.g., NGC 1399), so it is possible that starlight from an old population can account for half of the FUV continua. The remainder, if not most of the FUV continua, is probably due to young stars, as discussed by Mittaz et al. (2001) in their imaging study of the center of Abell 1795 with the optical monitor on *XMM*, which has UV channels.

When we scale the UV continuum of NGC 1399 to the region beyond 1110 Å (1044 Å in the rest frame), the two most significant features in the entire LiF2a spectrum occur at 1096.8 Å and 1106.4 Å. This first feature corresponds to the location of the strong O VI line at the redshift of the central galaxy and the optical emission line gas in Abell 1795. We believe that the second feature is associated with young hot stars that have been formed recently and create much of the UV continuum. There can be a few significant spectral differences for hot stars in this wavelength range (Pellerin et al. 2002; Walborn et al. 2002). The spectrum rises from the minimum caused by Lyβ absorption (1091 Å), although the feature is typically 10Å FWHM and damped, leading to the slow rise in both the young hot stars (Figure 4) and the old hot stars in NGC 1399 (Figure 3). Young hot stars can have a wind, and depending upon the mass flux, P-Cygni profiles can occur (Walborn et al. 2002), which causes the peak near 1104.5–1109.5 Å (1038.5–1043.5 Å in the rest frame), corresponding to the peak observed in the LiF2a spectrum. The weak O VI line is not apparent, but its wavelength corresponds to an absorption feature in an O/B star. If we subtract the hot star stellar atmosphere from the spectrum, an emission line would appear at the location of the O VI λ 1038 line, so it is possible that both lines exist.

In trying to determine the strength of the strong O VI line, we note that a strong Galactic Fe II absorption line would lie near the line center. Using the stellar continua as a baseline, we find that the line flux is 2.3×10^{-15} erg cm^{-2} s^{-1} ($\pm$ 0.6×10^{-15} erg cm^{-2} s^{-1}), with a line center at 1069.9 (z = 0.0630) and a line width of 2.3 Å FWHM. The absorption-corrected flux for the strong O VI line is 2.7×10^{-15} erg cm^{-2} s^{-1} ($\pm$ 0.7×10^{-15} erg cm^{-2} s^{-1}), and for a distance of 268 Mpc, the luminosity is 2.3×10^{40} erg s^{-1} ($\pm$ 0.6×10^{40} erg s^{-1}).

The O VI line emission from the central pointing was listed as an upper limit by Oegerle et al. (2001). Since that time, improvements in the pipeline processing have reduced the noise in the spectral extraction and our understanding of the underlying stellar continuum

has improved. There was also a concern of significant airglow contamination with the strong line from N_2 when pointing near the illuminated disk of the Earth, the strongest near the O VI line being at 1098.1 Å (there is a much stronger N_2 line at 1034 Å). In comparing the night-only data with the day-plus-night data, there is a tremendous reduction in the 1034 Å line, and a small fraction of the emission at 1098.1 Å decreases. Therefore, it is unlikely that the 1098.1 Å airglow line contributes significantly to the line, especially as it is to the red of the line defined by its FWHM.

Although it is not central to the primary science, the C III λ 977 line is detected in the LiF1a channel (Figure 5). It is the strongest feature in that channel not due to airglow and has a central wavelength of 1038.5 Å, with a flux of 4.2×10^{-15} erg cm^{-2} s^{-1} $\pm$ 0.5×10^{-15} erg cm^{-2} s^{-1}.

The observation for the off-center pointing of Abell 1795 was taken at two times in 2004, with total exposure times of 6.49 ksec and 18.86 ksec, although we are using only the night data since the background is significantly lower, leading to a higher S/N for the final spectra. The final useful night time data had exposure times of 4.48 ksec and 12.7 ksec or a total time of 17.2 ksec. We use the combined night spectrum for the analysis, in which the airglow lines from oxygen and nitrogen are so weak as to be undetectable.

The detector with the highest S/N in the wavelength region where the redshifted emission would occur is the LiF2a channel, and the strongest feature in this channel occurs at 1095.1 Å, which is approximately the redshifted wavelength of the O VI λ 1032 line, z = 0.06122 (Figure 6). This line is 370 km s^{-1} to the blue of the mean redshift of the cluster, which has a velocity dispersion of 810 km s^{-1} (Oegerle & Hill 2001). However, the optical emission line gas is also blueshifted at this location by 100-200 km s^{-1}, and the line width is broad and extends to the velocity of the O VI emission (Hu et al. 1985). This line is detected at the 3 σ level and with a flux of 1.4×10^{-15} erg cm^{-2} s^{-1} $\pm$ 0.5×10^{-15} erg cm^{-2} s^{-1}, and the FWHM is 1.0 $\pm$ 0.2 Å. The weaker O VI line, which is not detected, would have been a 1.5 σ feature. To be conservative, we view this as a possible detection and discuss it accordingly. A very faint stellar continuum is present as well, with a peak emission in the 1105-1120 Å range (1040-1053 Å in the rest frame), as expected for a hot stellar continuum from young stars; the zero point is too uncertain to place a secure flux level on the continuum. Another feature that one might expect, either from cooling gas or photoionized gas, is the C III λ 977 line, and there is a marginal detection of this line at the 2 σ level, 1.4×10^{-15} erg cm^{-2} s^{-1} $\pm$ 0.7×10^{-15} erg cm^{-2} s^{-1}.

2.3. AWM 7

The cluster AWM7 is a nearby X-ray bright cluster with an elliptical galaxy at the center, at a velocity of 5194 km s^{-1}. It lies at l, b = 146° -15.6° and the extinction is E(B-V) = 0.116 mag (Schlegel, Finkbeiner, and Davis 1998). It was observed on 26 September 2003 with a total exposure time of 21.1 ksec, but the S/N is highest when using the night-only data, which comprises 14.1 ksec.

The spectra show no features at all, aside from the usual Hβ airglow line. From the noise characteristics of the spectrum, we derive a 3σ upper limit of 3×10^{-15} erg cm^{-2} s^{-1} to an O VI line of width 300 km s^{-1}. After correction for extinction, the strong O VI line has an upper limit to its luminosity of 8×10^{39} erg s^{-1}.

3. Interpretation and Discussion

The OVI luminosities can be converted into mass cooling rates using radiative cooling models. Since these OVI lines carry the cooling through this temperature region, the line strength is the product of the thermal energy of the gas at $10^{5.5}$ K and the rate at which matter is cooling through that region (Edgar and Chevalier 1986; Voit, Donahue, and Slavin 1994). Factors such as the metallicity of the gas, departures from thermal equilibrium, and whether the gas is isochoric or isobaric only modify the line strength modestly. For the conversion from L(λ1032) to a mass cooling rate, we use the value discussed by Bregman, Miller, and Irwin (2001) (see Edgar and Chevalier 1986 and Voit, Donahue, and Slavin 1994), of $\dot{M}$ = (L(λ1032)/9×10^{38} erg s^{-1}) $M_\odot$ yr^{-1}. Using this conversion, the upper limit to the cooling rate for AWM 7 is 9 $M_\odot$ yr^{-1} within r = 6.1 kpc, and the detected cooling rate for Abell 426 is 32±5 $M_\odot$ yr^{-1} within the central r = 6.2 kpc. For Abell 426, the cooling radius is about an order of magnitude larger than the *FUSE* aperture and the optical emission line gas region is also considerably larger, so we may be missing much of the O VI emission. Therefore, we regard this cooling rate as a minimum value.

The cooling rate for the central pointing of Abell 1795 is about 26±7 $M_\odot$ yr^{-1} in the central r = 22 kpc region. If we treat the off-center pointing as a detection, it represents an additional 16±6 $M_\odot$ yr^{-1}, or a total measured in the cluster of 42±9 $M_\odot$ yr^{-1}. Once again, much of the cooling gas may not be contained within our apertures, so the total cooling rate for the cluster is likely to be larger.

We can compare our measurements with the three other rich clusters that have been observed with *FUSE*, Abell 2597, Abell 2029, and Abell 3112 (Oegerle et al. 2001; Lecavelier des Etangs et al. 2004). When we convert these published values to the same Hubble constant

and cooling rate scale, the upper limits for Abell 2029 and Abell 3112 are 27 $M_\odot$ yr^{-1} (r = 27 kpc), and 25 $M_\odot$ yr^{-1} (r = 26 kpc), while for Abell 2597, the detected value is 35 $M_\odot$ yr^{-1} (r = 30 kpc). In summary, of the six clusters observed, three are detected in the O VI lines.

There are other characteristics that distingish the clusters detected in O VI from those that were not. The three clusters, Abell 426, Abell 1795, and Abell 2597 have extensive optical emission lines and also have evidence for recent or ongoing star formation. Although the other galaxy clusters were considered cooling flow clusters from their broad-band X-ray data, they are not known to have optical emission line filaments or star formation, such as Abell 2029 (Hu et al. 1985; McNamara & O'Connell 1989, 1993; Cardiel et al. 1998). It had been suggested by others that the combination of peaked X-ray emission with short cooling times, optical emission line gas, and young stars constituted a strong case for the cooling flow paradigm (e.g., Cardiel et al. 1998). The counterargument was that the cooled gas was mass loss from a recently stripped galaxy, and the disturbance had led to star formation in the gas (Sparks et al. 1997). In this view, the gas does not cool from the hot ambient cluster medium. However, the presence of O VI emission shows that, at least in some clusters, gas is cooling through the $10^{5.5}$ K regime at a rate of at least 30 $M_\odot$ yr^{-1}. The original cooling flow estimates for these clusters are typically an order of magnitude larger. Either the O VI emission that we detected is only a fraction of the cooling gas, which is possible since the apertures cover only a fraction of the cooling flow region, or the cooling rate is an order of magnitude lower than originally estimated. A significantly lower cooling rate would, in general, be consistent with the weak X-ray cooling lines, and models have been developed along these lines (Soker & David 2003).

We can compare the cooling rates inferred from the O VI emission with the constraints from the X-ray data, and in particular, the *XMM* RGS data. There is not yet a published RGS spectrum for Abell 426, but there are analyses for both Abell 1795 and Abell 2597. The EPIC plus RGS spectrum for Abell 2597 implies an X-ray cooling rate of 50±10 $M_\odot$ yr^{-1} (adjusted for the H_0 used here) and a cooling radius of about 90 kpc (Morris & Fabian 2005). This cooling rate is somewhat greater than the value that we measure, suggesting that cooling gas may extend beyond the *FUSE* LWRS aperture. If the cooling rate increases linearly with radius out to the cooling radius, as suggested by theory (Fabian 1994), the value inferred from the *FUSE* data would become 50-60 $M_\odot$ yr^{-1}, the same as found from the X-ray data. The study that includes Abell 1795 (Peterson et al. 2003) places an upper limit to the cooling of 30 $M_\odot$ yr^{-1}, which may be in conflict with the O VI data that implies 30–40 $M_\odot$ yr^{-1}. If such a conflict exists, it would imply that non-steady cooling of material is involved, such as turbulent mixing layers (Slavin, Shull, and Begleman 1993), although there are other possibilities (Fabian et al. 2001).

This promising line of study of O VI emission is limited by the sensitivity of current instrumentation. Natural follow-up observations, such as the mapping of O VI throughout the potential cooling region will have to wait for future missions.

We would like to thank the *FUSE* team for their assistance in the collection and reduction of these data. Also, we would like to thank Birgit Otte and Renato Dupke for their comments and suggestions in writing this paper. This research has made use of the NASA/IPAC Extragalactic Database (operated by JPL, Caltech), the Multimission Archive at Space Telescope, and the NASA Astrophysics Data System, operated under contract with NASA. We gratefully acknowledge support by NASA through grants NAG5-9021, NAG5-11483, G01-2089, GO1-2087, GO2-3114, and NAG5-10765.

REFERENCES

Bregman, J.N., Miller, E.D., Athey, A.E., and Irwin, J.A. 2005, ApJ, submitted

Bregman, J.N., Miller, E.D., and Irwin, J.A. 2001, ApJ, 553, L125

Burstein, D., Bertola, F., Buson, L. M., Faber, S. M., & Lauer, T. R. 1988, ApJ, 328, 440

Cardelli, J. A., Clayton, G. C., & Mathis, J. S. 1989, ApJ, 345, 245

Cardiel, N., Gorgas, J., & Aragon-Salamanca, A. 1998, MNRAS, 298, 977

Conselice, C. J., Gallagher, J. S., & Wyse, R. F. G. 2001, AJ, 122, 2281

Cowie, L. L., Hu, E. M., Jenkins, E. B., & York, D. G. 1983, ApJ, 272, 29

Donahue, M., Mack, J., Voit, G. M., Sparks, W., Elston, R., & Maloney, P. R. 2000, ApJ, 545, 670

Edgar, R.J., and Chevalier, R.A. 1986, 310, L27

Edge, A. C., Wilman, R. J., Johnstone, R. M., Crawford, C. S., Fabian, A. C., & Allen, S. W. 2002, MNRAS, 337, 49

Fabian, A. C. 1994, ARA&A, 32, 277

Fabian, A. C., Sanders, J. S., Ettori, S., Taylor, G. B., Allen, S. W., Crawford, C. S., Iwasawa, K., & Johnstone, R. M. 2001, MNRAS, 321, L33

Fabian, A. C., Mushotzky, R. F., Nulsen, P. E. J., & Peterson, J. R. 2001, MNRAS, 321, L20

Ferruit, P., Adam, G., Binette, L., & Pecontal, E. 1997, New Astronomy, 2, 345

Hu, E. M., Cowie, L. L., & Wang, Z. 1985, ApJS, 59, 447

Hu, E. M., Cowie, L. L., Kaaret, P., Jenkins, E. B., York, D. G., & Roesler, F. L. 1983, ApJ, 275, L27

Irwin, J. A., Stil, J. M., & Bridges, T. J. 2001, MNRAS, 328, 359

Jaffe, W. 1990, A&A, 240, 254

Jaffe, W., Bremer, M. N., & Baker, K. 2005, ArXiv Astrophysics e-prints, arXiv:astro-ph/0504413

Jaffe, W., Bremer, M. N., & van der Werf, P. P. 2001, MNRAS, 324, 443

Krabbe, A., Sams, B. J., Genzel, R., Thatte, N., & Prada, F. 2000, A&A, 354, 439

Lecavelier des Etangs, A., Gopal-Krishna, & Durret, F. 2004, A&A, 421, 503

McNamara, B. R., & O'Connell, R. W. 1989, AJ, 98, 2018

McNamara, B. R., & O'Connell, R. W. 1992, ApJ, 393, 579

McNamara, B. R., & O'Connell, R. W. 1993, AJ, 105, 417

McNamara, B. R., O'Connell, R. W., & Sarazin, C. L. 1996, AJ, 112, 91

Minkowski, R. 1955, Carnegie Yearbook, 54, 25

Mittaz, J. P. D., et al. 2001, A&A, 365, L93

Morris, R. G., & Fabian, A. C. 2005, MNRAS, 358, 585

Norgaard-Nielsen, H. U., Hansen, L., & Jorgensen, H. E. 1990, A&A, 240, 70

Oegerle, W. R., Cowie, L., Davidsen, A., Hu, E., Hutchings, J., Murphy, E., Sembach, K., & Woodgate, B. 2001, ApJ, 560, 187

Oegerle, W. R., & Hill, J. M. 2001, AJ, 122, 2858

Pellerin, A., et al. 2002, ApJS, 143, 159

Peterson, J. R., Kahn, S. M., Paerels, F. B. S., Kaastra, J. S., Tamura, T., Bleeker, J. A. M., Ferrigno, C., & Jernigan, J. G. 2003, ApJ, 590, 207

Sabra, B. M., Shields, J. C., & Filippenko, A. V. 2000, ApJ, 545, 157

Sanders, J. S., Fabian, A. C., Allen, S. W., & Schmidt, R. W. 2004, MNRAS, 349, 952

Schlegel, D.J., Finkbeiner, D.P., and Davis, M. 1998, ApJ, 500, 525

Slavin, J.D., Shull, J.M., and Begleman, M.C. 1993, ApJ, 407, 83

Soker, N., & David, L. P. 2003, ApJ, 589, 770

Sparks, W. B., Carollo, C. M., & Macchetto, F. 1997, ApJ, 486, 253

Voit, G.M., Donahue, M., and Slavin, J.D. 1994, ApJS, 95, 87

Walborn, N. R., Fullerton, A. W., Crowther, P. A., Bianchi, L., Hutchings, J. B., Pellerin, A., Sonneborn, G., & Willis, A. J. 2002, ApJS, 141, 443

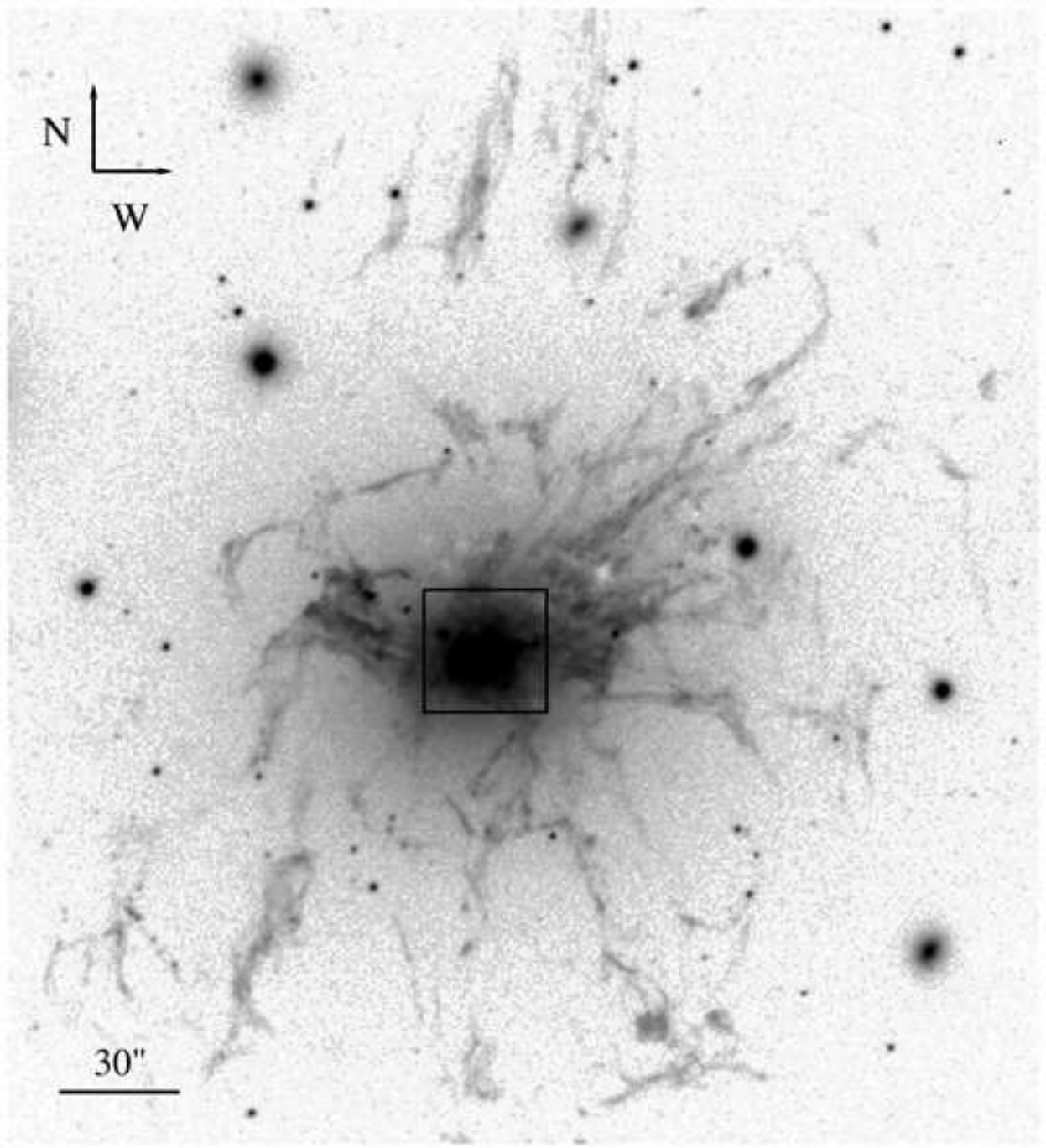

Fig. 1.— The *FUSE* LWRS aperture is superimposed upon the Hα image of Conselice et al. (2001), which shows the low velocity emission (5200 km s^{-1}) along with the continuum of NGC 1275 in Abell 426. The *FUSE* aperture only includes part of the extensive optical emission line gas.

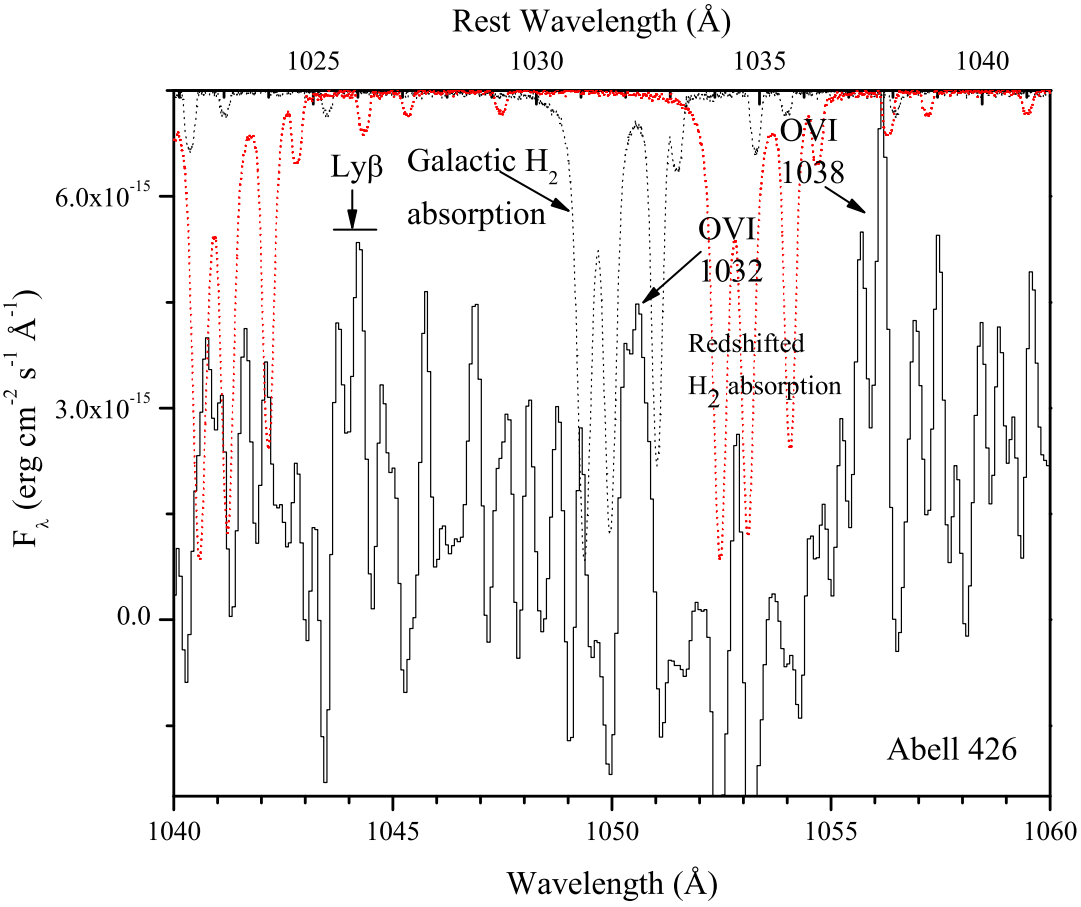

Fig. 2.— The *FUSE* spectrum of the center of Abell 426 shows both O VI emission lines plus a faint optical continuum and a Lyβ line. The rest wavelength is given at the top and the observed wavelength at the bottom. Galactic H_2 absorption (dotted black line) has probably absorbed some of the strong O VI line but the weaker line is unaffected. H_2 absorption within Abell 426 (dotted red line; 8200 km s^{-1}) is present but does not absorb the either O VI line.

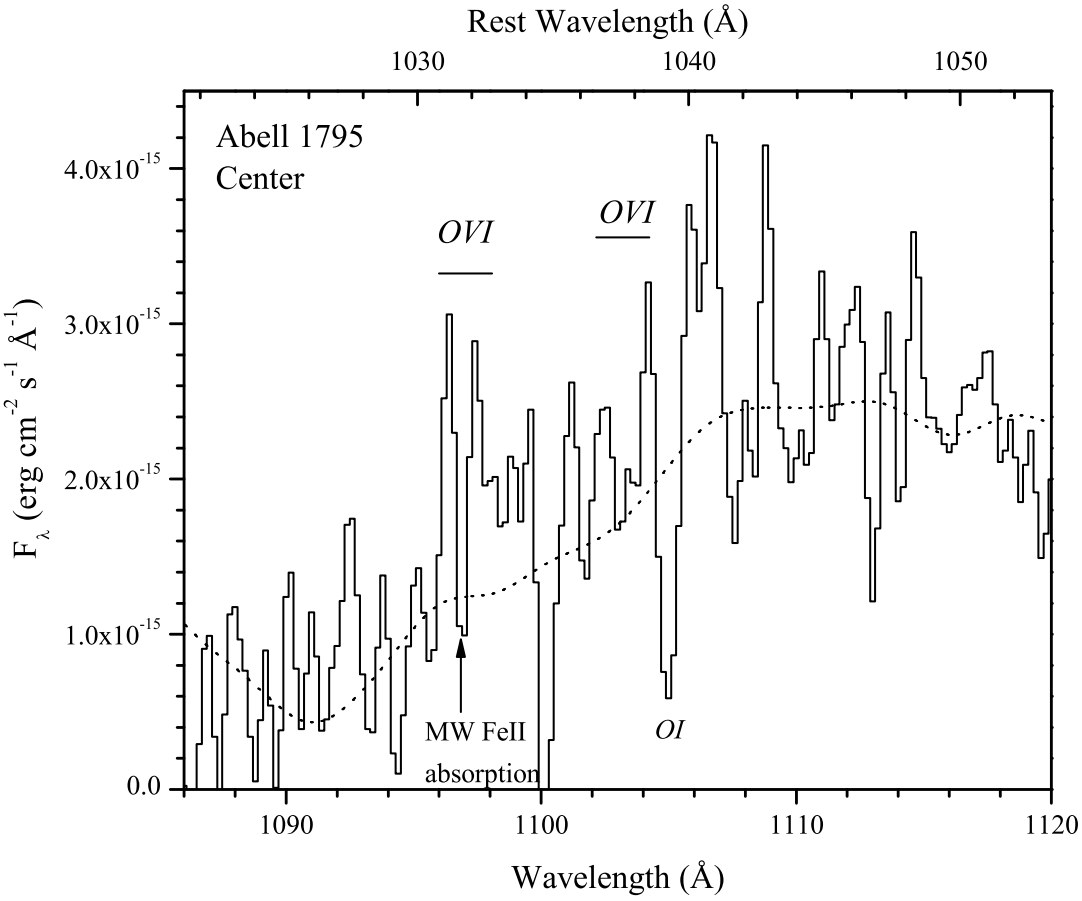

Fig. 3.— The *FUSE* LWRS spectrum of the center of Abell 1795, along with the continuum of the central galaxy of the Fornax cluster, NGC 1399 (dotted line), which has no emission lines (same wavelength scales as above). The strong O VI emission line lies above the continuum and is probably partly absorbed by a strong Galactic Fe II line at 1096.88 Å. The only other significant feature is emission at 1107 Å.

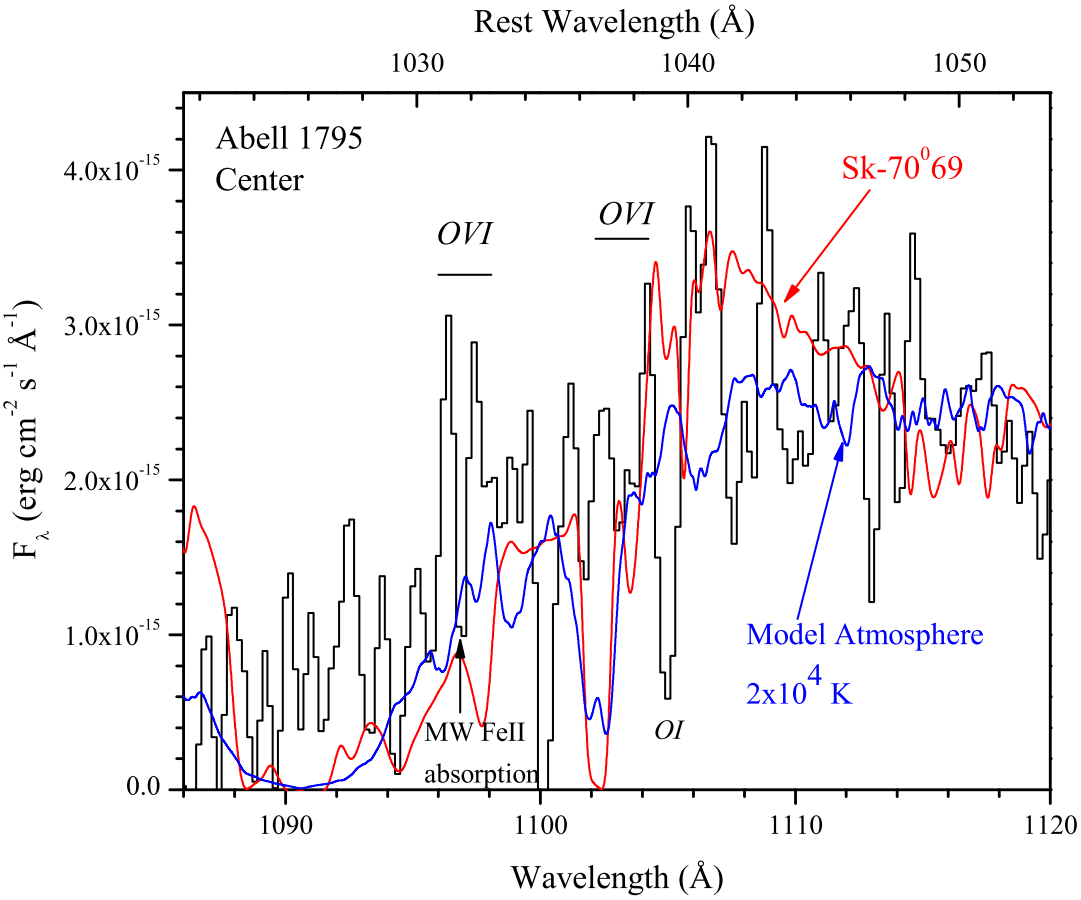

Fig. 4.— The same spectrum as above, except with the continuum of NGC 1399 replaced with the continuum of two hot stars, Sk-70°69 (red line; an O5V star showing a strong wind; Walborn et al. 2002), and a 2×10^4 K model atmosphere (log$g$ = 4; solar metallicity; blue line; we use the same wavelength scales as above). The star Sk-70°69 rises up to 1107 Å (1041 Å in the rest frame), which coincides with the peak in the observed spectrum from Abell 1795.

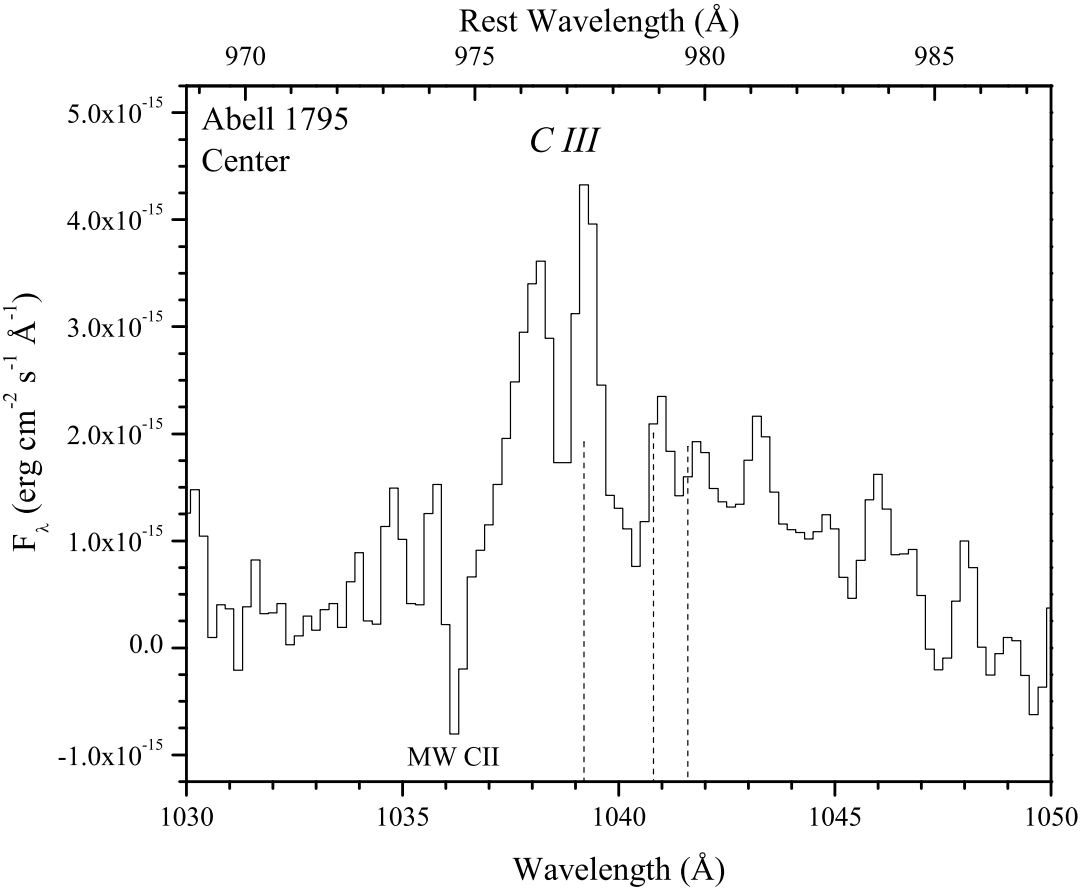

Fig. 5.— The spectral region containing the redshifted C III line in the central pointing of Abell 1795, along with markers of the location for airglow lines (vertical dashed lines), where the height of the dashed lines signifies the line relative strength. The red side of the C III line may have a small amount of contamination due to an airglow line.

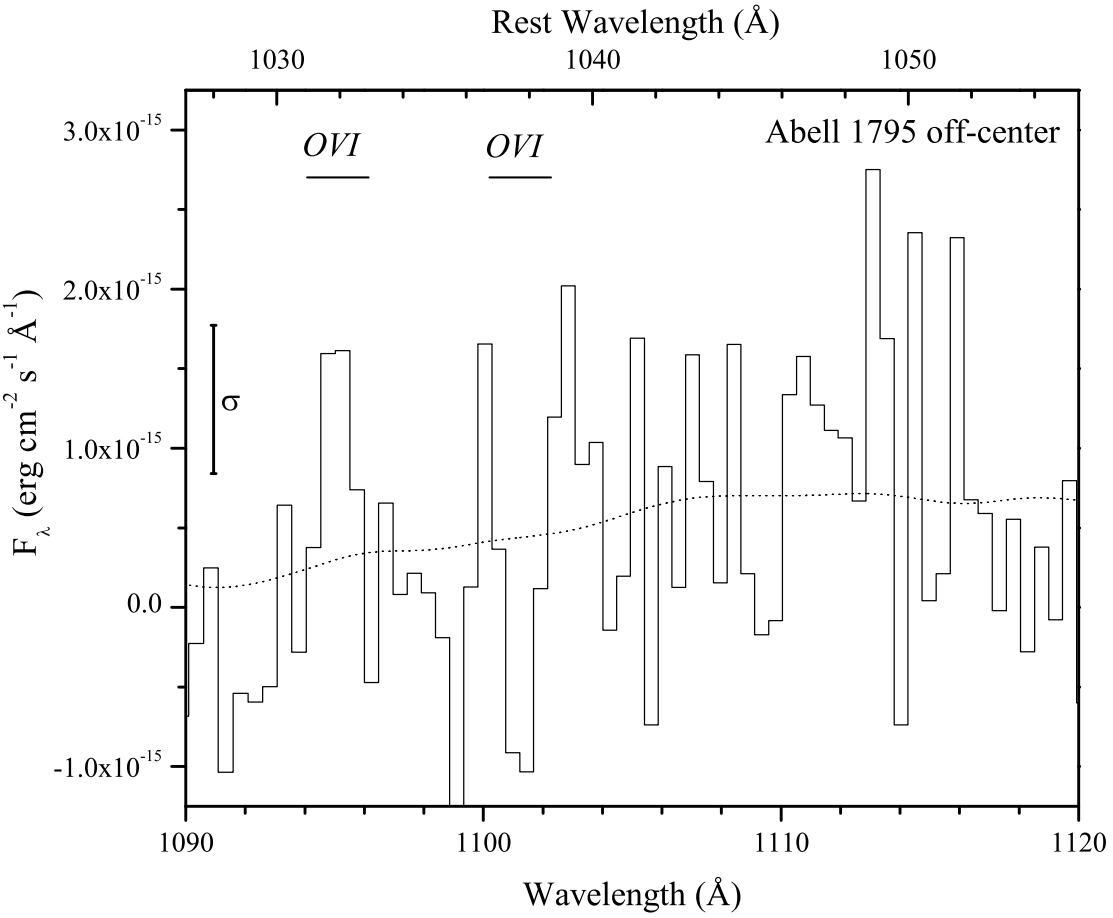

Fig. 6.— The *FUSE* LWRS spectrum taken 30″ from the center of Abell 1795, along with the continuum of NGC 1399 (dotted line). The strongest feature in this LiF2a spectrum is that of the strong O VI line, about a 3σ feature; the weaker O VI line is not detected.